Aluminosilicate-based adsorbent in equimolar and non-equimolar binary-component heavy metal removal systems

Meng Xu, Pejman Hadi, Chao Ning, John Barford, Kyoung Jin An and Gordon McKay

ABSTRACT

Cadmium (Cd) and lead (Pb) are toxic heavy metals commonly used in various industries. The simultaneous presence of these metals in wastewater amplifies the toxicity of wastewater and the complexity of the treatment process. This study has investigated the selective behavior of an aluminosilicate-based mesoporous adsorbent. It has been demonstrated that when equimolar quantities of the metals are present in wastewater, the adsorbent uptakes the Pb^{2+} ions selectively. This has been attributed to the higher electronegativity value of Pb^{2+} compared to Cd^{2+} which can be more readily adsorbed on the adsorbent surface, displacing the Cd^{2+} ions. The selectivity can be advantageous when the objective is the separation and reuse of the metals besides wastewater treatment. In non-equimolar solutions, a complete selectivity can be observed up to a threshold Pb^{2+} molar ratio of 30%. Below this threshold value, the Cd^{2+} and Pb^{2+} ions are uptaken simultaneously due to the abundance of Cd^{2+} ions and the availability of adsorption sites at very low Pb^{2+} molar ratios. Moreover, the total adsorption capacities of the adsorbent for the multi-component system have been shown to be in the same range as the single-component system for each metal ion which can be of high value for industrial applications.

Key words | binary-component adsorption, cadmium and lead removal, heavy metal separation, ion-exchange, mesoporous aluminosilicate-based adsorbent

Meng Xu
Pejman Hadi
Chao Ning
John Barford
Gordon McKay (corresponding author)
Chemical and Biomolecular Engineering Department,
Hong Kong University of Science and Technology,
Clear Water Bay Road,
Hong Kong SAR
E-mail: *kemckayg@ust.hk*

Pejman Hadi
Kyoung Jin An
School of Energy and Environment,
City University of Hong Kong,
Tat Chee Avenue,
Hong Kong SAR

Gordon McKay
Division of Sustainable Development, College of Science, Engineering and Technology,
Hamad Bin Khalifa University, Qatar Foundation,
Doha,
Qatar

INTRODUCTION

Heavy metals are found pervasively in soil and aqueous systems either naturally or as a result of anthropogenic human activities via agricultural, industrial and mining operations (Fu & Wang 2011). The presence of toxic heavy metals in excess quantities in the ecosystem has jeopardized the environmental sustainability and has posed particularly serious concerns regarding human health (Cheung *et al.* 2001; Sang *et al.* 2008). Hence, the removal of heavy metals from the environment, especially from the aquatic ecosystem, has received particular attention.

Among various wastewater treatment techniques, such as precipitation, coagulation–flocculation, adsorption, membrane filtration and solvent extraction (Mavrov *et al.* 2003; Chuah *et al.* 2005; Larous *et al.* 2005; Wan Ngah & Hanafiah 2008; Pang *et al.* 2011), adsorption has been regarded as a simple, effective and environmentally friendly remediation process for the removal of heavy metals from effluent.

Various adsorbents have been developed and modified for pollutant remediation among which activated carbon is the most widely used class of adsorbents (Kadirvelu *et al.* 2001; Kobya *et al.* 2005; Amuda *et al.* 2007). Although these materials are highly valued for their ability to remove dyes and organics from wastewater streams, they are comparatively inefficient for heavy metal sequestration in aqueous media. Ion exchange adsorbents/resins belong to another class of materials for the removal of heavy metal ions from wastewater (Dąbrowski *et al.* 2004). The ions, usually alkali metals or alkaline earth metals, bound to the charged groups on the surface of the ion-exchangers, can be exchanged with heavy metals possessing higher electronegativity values. Despite the high efficiency of ion exchange materials for heavy metal-laden

doi: 10.2166/wst.2015.440

wastewater treatment, their high cost is a major drawback. Accordingly, many researches have been devoted to the possibility of the utilization of natural mineral compounds, such as clays (Veli & Alyüz 2007), vermiculite (Malandrino *et al.* 2006) and soils (Bradl 2004) which exhibit ion exchange behavior. Nevertheless, their low metal uptake capacities hinder their widespread application in industry. In order to overcome the cost challenge while retaining high efficiency, it seems feasible to consider the employment of waste materials as precursors to produce adsorbents/ion exchangers. While numerous studies concerning the utilization of agricultural and industrial waste to produce activated carbon have been conducted, only limited reports have focused on aluminosilicate-based waste utilization as potential adsorbents/ion exchangers, most of which converted fly ash remaining after the combustion of coal to various types of zeolites as ion exchangers for wastewater treatment applications (Shih & Chang 1996; Apiratikul & Pavasant 2008; Wang *et al.* 2008; Qiu & Zheng 2009; Sočo & Kalembkiewicz 2013). Jo *et al.* used a mixture of bottom ashes from a power plant and dredged soil, as a mesoporous material, for heavy metal removal from wastewater (Jo *et al.* 2014). Also, chemically modified waste glass from cathode ray tubes was employed as an adsorbent to remove Pb^{2+} ions from wastewater (Pant & Singh 2013). Nevertheless, the metal adsorption capacities of these waste materials were found to be low in most of the cases, which restrains their practical applications in industrial wastewater treatment applications. The production of low-cost, efficient adsorbents from waste entails two-fold ecological advantages; transformation of burdensome waste materials into value-added products and their utilization for pollutant-laden wastewater treatment.

Hadi *et al.* (2015b) have produced a mesoporous-structured adsorbent material (Hadi *et al.* 2015a) from the nonmetallic fraction (NMF) of waste printed circuit boards and demonstrated its high efficiency in heavy metal adsorption in single-component systems (Hadi *et al.* 2013b, 2014). Although the simultaneous presence of two toxic heavy metals, such as Cd^{2+} and Pb^{2+}, from various industrial wastewater is a common practice, only a few studies have dealt with the removal of Cd^{2+} and Pb^{2+} ions in binary systems. Also, to our best knowledge, the adsorption of non-equimolar heavy metals in multi-component systems has not been examined.

Hence, this research aims at studying the adsorption behavior of the activated waste PCB-derived adsorbent for the removal of Pb^{2+} and Cd^{2+} ions in single- and binary-component systems at various concentrations, pH values and adsorbent dosages. Also, since it is believed that the molar ratio of the metals present in wastewater affects the selectivity of the adsorbent, both equimolar and non-equimolar binary systems have been examined and the effect of metal ratio in selective behavior of the adsorbent material has been discussed.

EXPERIMENTAL

Materials

A local company in Hong Kong provided the micron-sized NMF (average particle size of 2 μm) as raw material. Potassium hydroxide (KOH, >85%), cadmium nitrate tetrahydrate ($Cd(NO_3)_2.4H_2O$, >99%) and lead nitrate ($Pb(NO_3)_2$, >99%) were purchased from Sigma-Aldrich Company, UK.

Adsorbent preparation and characterization

The adsorbent material was prepared according to the procedure described in our previous work (Hadi *et al.*; Xu *et al.* 2014), using KOH as activating agent. The raw material, NMF, was impregnated with the activating agent at a weight ratio of 2:1 (KOH:NMF) with continuous stirring for 3 h at room temperature. After the mixing was completed, the slurry with deagglomerated NMF particles was transferred to a muffle furnace and heated to 250 °C at a rate of 5 °C min^{-1} for 3 h under a nitrogen atmosphere (purity > 99.99%). Then, the furnace was cooled down to room temperature. The resultant material was washed with boiling water several times until the supernatant liquor was clear. Afterwards, the supernatant was drained and the activated material (A-NMF) was dried at 110 °C and stored in a desiccator for later experiments.

The textural properties and the surface chemistry of NMF and A-NMF were examined using a Coulter SA 3100 surface area analyzer by the nitrogen gas adsorption-desorption technique at 77 K after outgassing at 150 °C for 1 h, a PerkinElmer GX 2000 Fourier transform infrared spectroscopy (FTIR) and elemental analyzer. In addition, X-ray photoelectron spectroscopy (XPS, Physical Electronics PHI 5000) was used to investigate the surface atomic concentration of the materials.

Adsorption studies

Single- and binary-component adsorption of Pb^{2+} and Cd^{2+} ions was carried out to evaluate the adsorption behavior and capacity of the prepared activated material, A-NMF, under various conditions.

In a single-component system, 50 mL of metal solutions with initial concentrations in the range of 0.5 to 7 mmol.L^{-1} and a pH level 4 were placed in plastic bottles containing 50 mg adsorbent material and kept in a shaker at 150 rpm at a constant temperature of 25 °C. After the adsorption equilibrium was reached, the final pH values of the solutions were measured and the samples were withdrawn and filtered. Both initial and final metal concentrations of the solutions were analyzed by inductively coupled plasma atomic emission spectroscopy (ICP-AES, Optima 7300 DV, Perkin-Elmer, USA). The metal adsorption capacities of the adsorbent were calculated using the metal mass balance in aqueous and solid phases:

$$(q_e - q_o) \times m = (C_o - C_e) \times V \quad (1)$$

where q_0 is the amount of metal on fresh adsorbent (mmol.g^{-1}); q_e is the equilibrium metal adsorption capacity (mmol.g^{-1}); V is the volume of the metal solution (L); m is the amount of adsorbent used (g); C_0 and C_e are the initial and equilibrium concentrations of metal ions in the solution (mmol.L^{-1}), respectively.

For fresh adsorbent, no metal is present on the adsorbent surface, thus $q_0 = 0$. Therefore, Equation (1) can be rearranged as (Rouquerol *et al.* 1999):

$$q_e = \frac{(C_o - C_e)\,V}{m} \quad (2)$$

The effect of pH on the adsorption behavior of the adsorbent-adsorbate system was studied by varying the initial pH value of the metal solution from 2 to 6 at a constant initial metal concentration of 5 mmol.L^{-1}.

Similar adsorption experiments were employed for the binary-component system.

Single- and binary-component equilibrium models

Various single- and binary-component adsorption models were applied to fit the adsorption isotherms. The models used in this study have been summarized in Table 1.

Table 1 | Summary of adsorption models applied in this study

Model	Assumptions	Equation	Parameters
Langmuir	- Monolayer adsorption onto a homogeneous surface - Fixed and localized sites - No interaction between molecules	$q_e = \frac{K_L C_e}{1 + a_L C_e}$	K_L, a_L
Freundlich	- Multilayer adsorption onto a heterogeneous surface - Adsorption sites are not identical - Energy distribution decays exponentially	$q_e = a_F C_e \frac{1}{n}$	a_F, $\frac{1}{n}$
Sips (Langmuir–Freundlich)	- The adsorbate occupies two sites - n accounts for heterogeneity system and when $n = 1$, the equation approaches Langmuir - At low concentration the equation reduces to the Freundlich equation and does not obey Henry's Law	$q_e = \frac{K_{LF} C_e^{n_{LF}}}{1 + a_{LF} C_e^{n_{LF}}}$	K_{LF}, a_{LF}, n_{LF}
Redlich–Peterson	- Same as the Langmuir model	$q_e = \frac{K_{RP} C_e}{1 + a_{RP} C_e^{\beta_{RP}}}$	K_{RP}, a_{RP}, β_{RP}
Extended Langmuir	- Homogeneous surface with respect to the energy of adsorption - No interaction between adsorbed species - All adsorption sites are equally available to all adsorbed species	$q_{e,i} = \frac{K^0_{L,i} C_{e,i}}{1 + \sum a^0_{L,i} C_{e,i}}$	$K^0_{L,i}$, $a^0_{L,i}$
Extended Redlich–Peterson	- Same as the extended Langmuir model	$q_{e,i} = \frac{K^0_{RF,i} C_{e,i}}{1 + \sum a^0_{RP,i} C_{e,i}^{\beta^0_{RP,i}}}$	$K^0_{RF,i}$, $a^0_{RP,i}$, $\beta^0_{RP,i}$
Modified extended Freundlich equation	- Same as the Freundlich model	$q_{e,1} = \frac{K^0_{F,1} C_{e,1}^{n_1+n_{11}}}{C_{e,1}^{n_{11}} + a_{12} C_{e,2}^{n_{12}}}$ $q_{e,2} = \frac{a^0_{F,2} C_{e,2}^{n_2+n_{22}}}{C_{e,2}^{n_{22}} + a_{21} C_{e,1}^{n_{21}}}$	n_{11}, n_{12}, n_{22}, n_{21}, a_{12}, a_{21}

The calculated adsorption capacity, q_{cal}, was compared with the experimental adsorption capacity, q_{exp}, for each isotherm model. The sum of the squared errors (*SSE*) was used as the error function in this study and was calculated using Equation (3). The model parameters were determined to minimize the *SSE* values via the solver add-in function in Microsoft Excel which functions by applying an iterative method to find the optimum variables by minimizing the error function. The model with the least *SSE* value was selected as the best-fit model.

$$SSE = \sum (q_{exp} - q_{cal})^2 \quad (3)$$

RESULTS AND DISCUSSION

Material characterization

The detailed characterization of the original and modified materials has been reported in our previous works (Hadi *et al.* 2013a, b). Table 2 shows the Brunauer–Emmett–Teller (BET) surface area and pore volume of NMF and A-NMF determined by nitrogen gas adsorption–desorption technique. As seen in this table, the raw material, NMF, is non-porous with a surface area below 1 $m^2.g^{-1}$, while the A-NMF has a surface area of 222 $m^2.g^{-1}$ which demonstrates that the activation process has resulted in successful development of a porous structure. The comparison of the developed surface area for A-NMF with the reported values for fly ash, which has a similar structure to NMF, shows that this surface area is either in the same range as the zeolites produced by fly ash using sophisticated processes (Pizarro *et al.* 2015; Zhou *et al.* 2015) or higher than the fly ash-based adsorbents produced (Kostova *et al.* 2013; Duta & Visa 2015; Itskos *et al.* 2015; Norris *et al.* 2015; Ogata *et al.* 2015). Also, the pore volumes show that the activated material mainly consists of mesopores. Based on CHNS elemental analysis, NMF contains more than 20% carbon in its structure while the carbon content of the A-NMF is found to be less than 2%. This shows that carbon has been burned off after the activation process. Carbon burn-off at such a low temperature has been related to the catalyzing effect of the presence of potassium and calcium (Yuan *et al.* 2011; Hadi *et al.* 2013c). Moreover, the XRF analysis demonstrates that the major composition of the A-NMF is silicon, aluminum and calcium originating from calcium aluminosilicate, a material commonly used as an adsorbent for wastewater treatment.

The chemistry of the adsorbent surface was examined by FTIR. Figure 1 shows the FTIR spectra of both NMF and A-NMF. The spectrum of A-NMF displays a strong, broad signal between 3,250 and 3,550 cm^{-1}, which is attributed to the presence of hydroxyl groups ($^{-}$OH), whereas no hydroxyl group can be found before the activation process. This indicates that the dominant activation mechanism is the cleavage of the siloxane groups to form the silanol groups on the surface of the adsorbent. The peak located at 1,013 cm^{-1} is assigned to the siloxane groups. This increase in the intensity of this peak after the activation has been related to the opening of the aluminosilicate tetrahedral cage which leads to the exposure of more siloxane groups to the surface of the material, consistent with pore development during the activation process. The XPS results also show the increase in the surface concentrations of silicon and oxygen groups confirming the FTIR results. Also, the existence of potassium ions on the surface of the adsorbent material, verified by XPS, confirms the successful doping of potassium ions which can potentially be exchanged with heavy metal ions.

Table 2 | Textural properties of the raw material, NMF, and activated material, A-NMF

Sample	S_{BET} $m^2.g^{-1}$	V_{mic} $cm^2.g^{-1}$	V_{meso} $cm^2.g^{-1}$	V_{tot} $cm^2.g^{-1}$	p/p_0
NMP	0.9	0.006	0	0.006	0.98
A-NMP	222	0.004	0.738	0.742	0.98

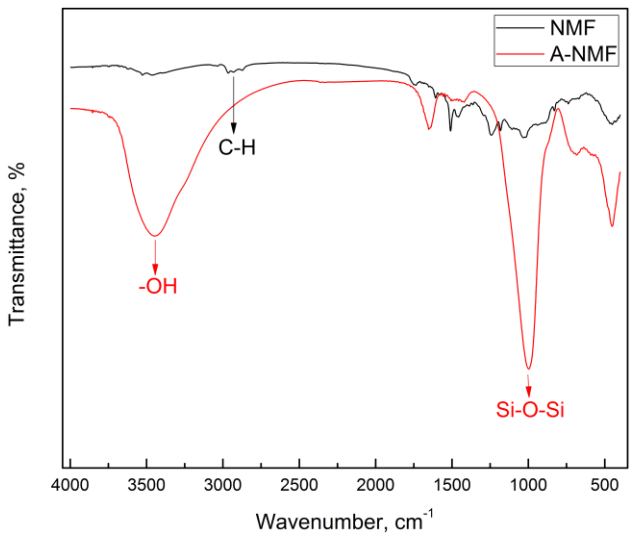

Figure 1 | FTIR spectra of NMF and A-NMF.

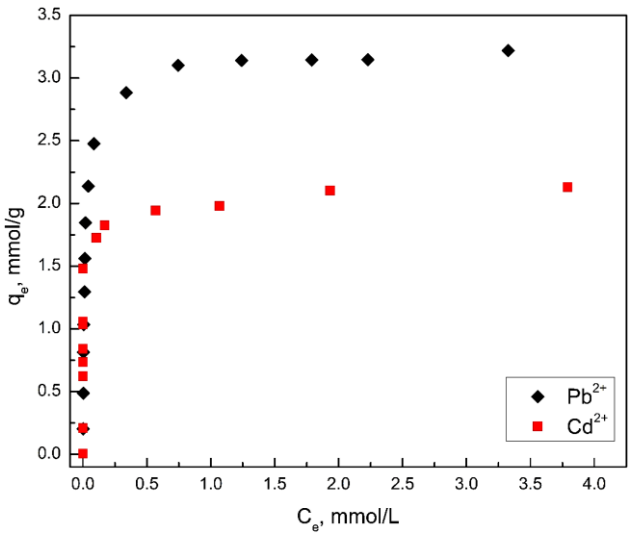

Figure 2 | Single component adsorptions of Pb^{2+} and Cd^{2+} by A-NMF. Experimental conditions: 50 mL metal solution, pH = 4, initial metal concentration = 0.5–7 mmol L^{-1}, 0.05 g adsorbent, equilibrium time = 5 days.

Single-component adsorption

Single component equilibrium isotherms for the adsorption of Pb^{2+} and Cd^{2+} ions using A-NMF are shown in Figure 2. A-NMF is capable of both Cd^{2+} and Pb^{2+} ion uptake with high adsorption capacities.

The uptake is mainly coordinated by the functional groups present on the adsorbent surface and its porous structure. The preliminary adsorption results demonstrated that the untreated material (NMF) does not uptake any metal ion. This is because of the trivial surface area of the adsorbent and the existence of no active functional groups on its surface. However, the activated material A-NMF which has a well-defined mesoporous network with functionalized surface can uptake the single-component metal ions with high adsorption capacities of 3.2 mmol.g^{-1} for Pb^{2+} and 2.1 mmol.g^{-1} for Cd^{2+}, showing higher affinity of this adsorbent material towards Pb^{2+} ion compared to Cd^{2+} ion. The comparison of these results with the adsorption capacities found in literature and the adsorption capacities of several commonly used commercial resins, summarized in Table 3, verifies the high efficiency of A-NMF as an adsorbent material to remove metal ions from effluents.

The single component adsorption isotherms are modeled using Langmuir, Freundlich, Sips (Langmuir–Freundlich) and Redlich–Peterson equations. The model parameters obtained to minimize the *SSE* together with the corresponding *SSE* values for all the isotherm equations are given in Table 4. Comparison of the *SSE* values for various model isotherms reveal that the Redlich–Peterson model shows the best fit to the experimental data for both Pb^{2+} and Cd^{2+} ions.

It is interesting to note that the Redlich–Peterson power constant, β_{RP}, for both Pb- and Cd-containing systems approaches unity, which reduces the Redlich–Peterson equation to the Langmuir model. Accordingly, it can be concluded that these adsorbent–adsorbate systems exhibit Langmuirian behavior. The Langmuir adsorption model is based on the assumptions that the adsorption occurs at a fixed number of definite, localized and equivalent sites and each site can only hold one molecule. According to this hypothesis, there will be no interaction between the adsorbed molecules, even on adjacent sites. So the molecules are bound to the surface of the available neighboring sites and this explains the limitation of the maximum capacity even at higher solution concentrations. However, the experimental data do not completely fit the Langmuir isotherm and exhibit a slight deviation, implying that not all sites represented homogeneous ion exchange with identical ions. The heterogeneity originates from the fact that the adsorption is not only mediated by ion exchange with potassium ions, but also physisorption is involved in the adsorption process, which causes the surface to behave in a slightly heterogeneous manner. Although the mechanism cannot be completely described by the Langmuir assumption, the uptake seems to obey monolayer adsorption behavior since the metal ion is the only species that can bond with the functional groups on the adsorbent surface in the solution and multilayer adsorption may be inhibited by the repulsion force between the aqueous and adsorbed heavy metal ions. The fits of various models are shown in Figure 3 for comparison.

Equimolar binary-component adsorption

The binary adsorption isotherm of the Pb^{2+} and Cd^{2+} ions using A-NMF is shown in Figure 4. According to this figure, Pb^{2+} ions are preferentially adsorbed by A-NMF from the equimolar Pb^{2+}–Cd^{2+} system. At low initial metal concentrations, the adsorbent material adsorbs Pb^{2+} and Cd^{2+} ions simultaneously due to the profusion of available adsorption sites. With an increase in the metal concentration, Pb^{2+} displaces the Cd^{2+} ions and occupies all the available sites, leaving Cd^{2+} in solution. Considering that the dominant mechanism in this system is ion exchange on the surface of the adsorbent material, this selective behavior is believed to originate from the difference in the electronegativities of the two metal ions. Pb (2.33) has a

Table 3 | Comparison of the adsorption capacities of A-NMF with reported adsorbents and commonly used commercial resins

Adsorbent/Resin	Adsorption capacity mmol.g^{-1}	Reference
Cadmium removal		
Present work	2.1	–
Hydroxyapatite	1.618	Corami *et al.* (2008)
Amberlite IR 120	0.9	Demirbas *et al.* (2005)
Activated carbon derived from bagasse	0.338	Mohan & Singh (2002)
Synthetic zeolite A	1.85	El-Kamash *et al.* (2005)
Sodium bicarbonate modified sugarcane bagasse	1.68	Karnitz *et al.* (2007)
Pleurotus sapidus	1.13	Yalçinkaya *et al.* (2002)
Sawdust (cedrus deodar wood)	0.65	Memon *et al.* (2007)
Cassava tuber bark waste	0.23	Horsfall *et al.* (2006)
Sulfuric acid-treated wheat bran	0.90	Özer & Pirinççi (2006)
Spent grain	0.15	Low *et al.* (2000)
Citric acid treated corncob	0.49	Leyva-Ramos *et al.* (2005)
α-Ketoglutaric acid-modified magnetic chitosan	1.79	Yang *et al.* (2014)
Lead removal		
Present work	3.2	–
Magnetic chitosan/graphene oxide composites	0.36	Fan *et al.* (2013)
Activated carbon	0.13	Momčilović *et al.* (2011)
Carbon nanotubes	0.49	Kabbashi *et al.* (2009)
Amberlite IR 120	0.41	Demirbas *et al.* (2005)
Rice husk	0.58	Wong *et al.* (2003)
Peanut husk	0.14	Li *et al.* (2007)
Polymerized banana stem	0.44	Noeline *et al.* (2005)
Spent grain	0.17	Low *et al.* (2000)
Sodium bicarbonate modified sugarcane bagasse	0.96	Karnitz *et al.* (2007)
Medicago sativa (alfalfa) biomass	0.43	Tiemann *et al.* (2002)
Treated *Azolla filiculoides* with $H_2O_2/MgCl_2$	1.1	Taghi ganji *et al.* (2005)
Hydrogen peroxide bagasse fly ash	0.012	Gupta & Ali (2004)

higher electronegativity compared to Cd (1.69) resulting in higher attraction of the Pb^{2+} ions to the negatively charged functional groups. This difference between the electronegativities of the two metals accounts for the higher affinity of the adsorbent material to the Pb^{2+} uptake which is more prone to compensate for its electron deficiency. The selective behavior of an adsorbent in a multi-component system can find significant applications, especially for the recovery and reuse of an individual metal from a multi-component medium.

As discussed in the previous section, the Langmuir-type isotherm properly described the rectangular-shape isotherm in the single-component systems. So the Langmuir-based multi-component models, extended-Langmuir and extended Redlich–Peterson models, were analyzed using two sets of Langmuir/Redlich–Peterson isotherm parameters obtained by the single-component modelling. However, both of these multi-component models fail to fit the experimental data in the binary-component system. This can be expected due to the selective behavior of the adsorbent in the Pb^{2+}–Cd^{2+} binary component. Indeed, extended Langmuir and extended Redlich–Peterson models are ideal isotherm models which assume that no interaction takes places between the components present in the adsorption medium. However, the competition between the two metal ions evidently verifies the occurrence of significant interaction between these two species, resulting in the non-ideality of the adsorption system. Moreover, the limitation of the model equation is

Table 4 | Model parameters of single component metal adsorption using A-NMF

Model	Parameter	Unit	Pb^{2+}	Cd^{2+}
Langmuir	K_L	$L\ g^{-1}$	205	88.8
	a_L	$L\ mmol^{-1}$	64.6	42.6
	SSE	–	0.358	0.0125
Freundlich	a_F	$mmol \cdot g^{-1} \cdot (L \cdot mmol^{-1})^{\frac{1}{n}}$	2.76	1.99
	$\frac{1}{n}$	–	0.150	0.057
	SSE	–	2.94	0.0034
Sips (Langmuir–Freundlich)	K_{LF}	$mmol \cdot g^{-1} \cdot (L \cdot mmol^{-1})^{n_{LF}}$	84.4	8.15
	a_{LF}	$(L \cdot mmol^{-1})^{n_{LF}}$	57.7	3.06
	n_{LF}	–	0.804	0.214
	SSE	–	0.248	0.0028
Redlich–Peterson	K_{RP}	$L \cdot g^{-1}$	256	343
	a_{RP}	$(L \cdot mmol^{-1})^{\beta_{RP}}$	82.5	170
	β_{RP}	–	0.966	0.955
	SSE	–	0.224	0.0026

another reason for lack of appropriate fitting in the multi-component system. When there is selectivity in the binary-component system, even the constant $K^0_{L,Pb}$ is larger than $K^0_{L,Cd}$, the equilibrium concentration of Pb^{2+} is far less than that of Cd^{2+}. Since the numerators of these extended models are formed by multiplication of $C_{e,i}$ and $K^0_{L,i}$, the extended Langmuir-based models can only provide reasonable estimates for multi-component systems as long as the C_e values of the metal ion present in multi-component systems are close to each other, that is when the adsorption follows a simultaneous trend, not a selective trend.

Since predictive models assuming an ideal system are not effective in modeling this binary-component system, the modified extended Freundlich model as a non-ideal model with a heterogeneity factor has been used to fit the data. The extended Freundlich isotherm was originally proposed by Fritz and Schlunder (Fritz & Schlunder 1981). Later on, McKay and Al-Duri modified the evaluation of correlation factors so as to reduce the extensive calculation procedure (McKay & Al-Duri 1991). They obtained appropriate agreement between the experimental and calculated data for a dye/carbon system (Al-Duri *et al.* 1992). It is a method highly recommended for systems with significant non-ideal effects and heterogeneous surfaces. Figure 5 shows that the modified extended Freundlich model can correlatively predict the observed experimental data for this binary-component system.

Several literature have reported a decrease in the equilibrium adsorption capacity of the adsorbent in multi-component systems. Kadirvelu *et al.* (2008) have observed that co-adsorption of Pb^{2+} and Cd^{2+} induces a drastic decrease in the adsorption capacity. Chiban *et al.* (2011) have also reported a reduction in the adsorption capacity of the adsorbent in a binary-component Pb^{2+}–Cd^{2+} system. This trend has also been observed by several other researchers (Entezari & Soltani 2009). In this study, the added-up capacity of the adsorbent in the equimolar system is similar to that of the single-component system for Pb^{2+} which suggests a strong interaction between the adsorbent active sites and both of the adsorbates. Hence, the efficiency of the adsorbent will not be sacrificed by the presence of other metal ions.

Non-equimolar binary-component adsorption

Since selectivity has been observed in the equimolar binary-component system, the effect of different metal ratios on the selectivity of the adsorption is of importance, since depending on the dominance of the metal ion in the solution, the selective behavior of an adsorbent may change to simultaneous behavior. Adsorption capacities, q_e, for each metal ion have been determined at various Cd^{2+}:Pb^{2+} ratios and are plotted against the molar ratio of Pb^{2+}, the more dominant species in this case. The molar ratio of Pb^{2+} is defined as the molar ratio of the Pb^{2+} concentration over the total metal concentration. As illustrated in Figure 6, it is observed that when the Pb^{2+} ion is at low Pb^{2+} molar ratio (below 30%), the other metal will have the chance to be adsorbed simultaneously due to its higher concentration and thus higher probability of contact between Cd^{2+} ions and the active adsorption sites. Once the concentration ratio of Pb^{2+} ions is above the threshold concentration of 30%, the adsorbent material, A-NMF, exhibits complete selective

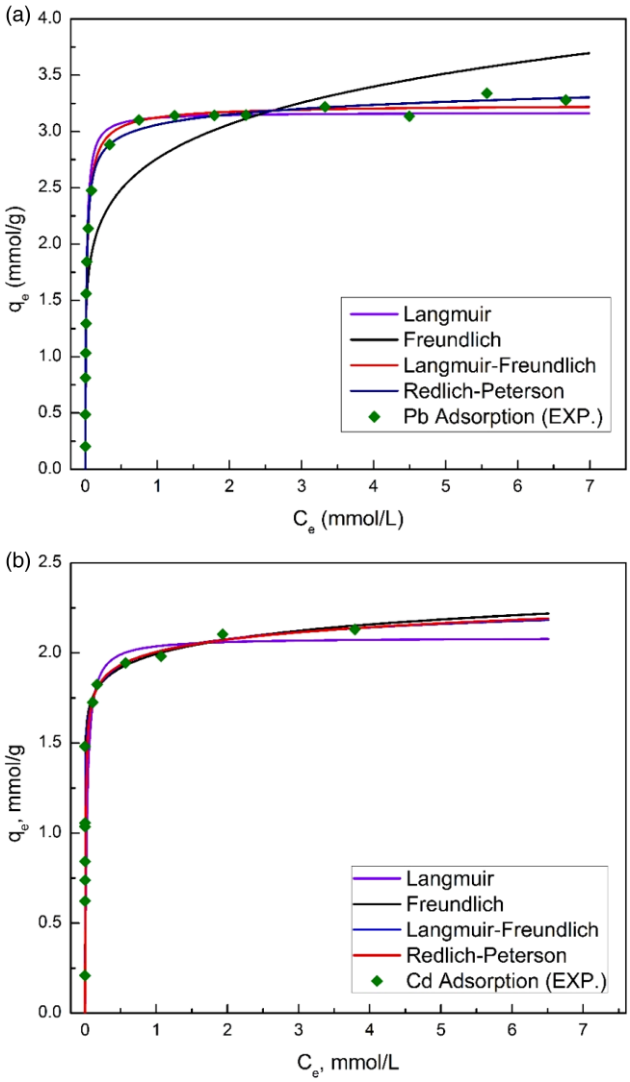

Figure 3 | Model fitting with various adsorption models to single-component adsorption of (a) Pb^{2+} and (b) Cd^{2+} by A-NMF.

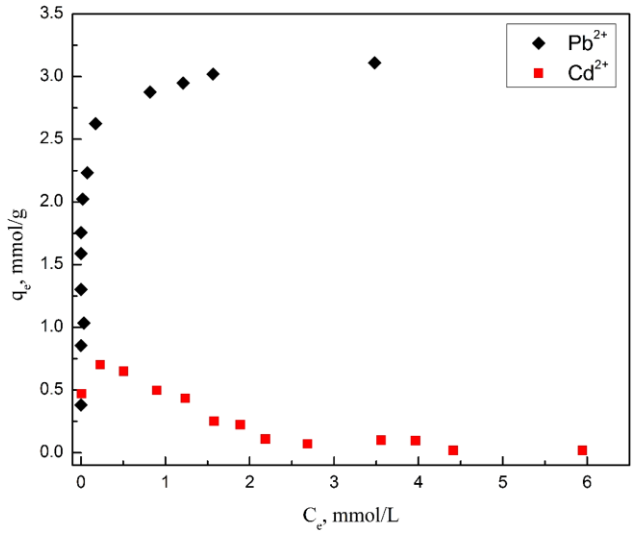

Figure 4 | Equimolar binary adsorption of Pb^{2+} and Cd^{2+} by A-NMF. Experimental conditions: 50 mL metal solution initial pH = 4, initial concentration for each metal = 0.5–6 mmol L^{-1}, Pb^{2+}:Cd^{2+} = 1, 0.05 g adsorbent, equilibrium time = 5 days.

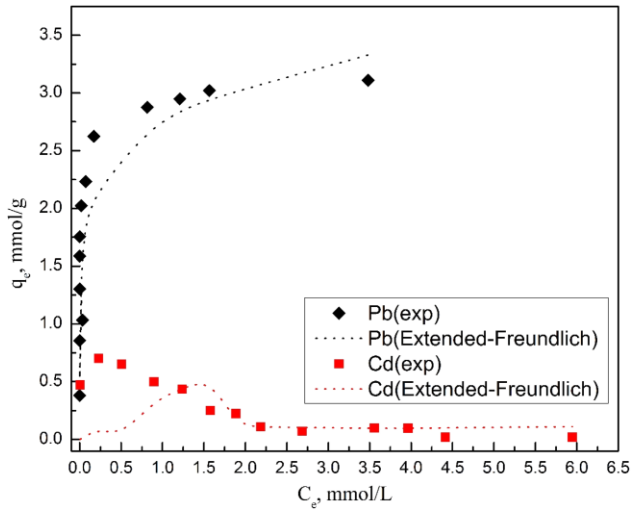

Figure 5 | Fit of the modified extended Freundlich adsorption model to Pb^{2+}–Cd^{2+} binary-component system.

adsorption behavior towards the Pb^{2+} ions implying the drastic effect of the electronegativity compensating for the lower Pb^{2+} concentration in a range of 30–50%. This selectivity is evidently retained with the increase of the Pb^{2+} molar ratio above 50%, where by the electronegativity and higher Pb^{2+} content have additive effects.

In order to investigate the behavior of the binary system at different total metal concentrations when the dominant Pb^{2+} species is at low Pb^{2+} molar ratio, the capacities against equilibrium concentrations with different metal ratios are shown in Figure 7(a)–(c). At metal ratios of Cd^{2+}:Pb^{2+} = 6:4 and 7:3, when the total metal concentrations are low, there are unoccupied adsorption sites readily available to adsorb the competing Cd^{2+} ions, together with the dominant Pb^{2+} ions. By increasing the total concentration of the metal ions, displacement takes place as Pb^{2+} ions, the dominant species, displaces the Cd^{2+} ions on the surface of the adsorbent, resulting in the inhibition of the Cd^{2+} uptake.

However, according to Figure 7(c), where the Pb^{2+} ions only account for 20% of the total metal concentration, the Cd^{2+} ions are not fully displaced by the Pb^{2+} ions during the adsorption process even at high total metal concentrations. This is because of the low Pb^{2+} concentrations leaving abundant available adsorption sites for the

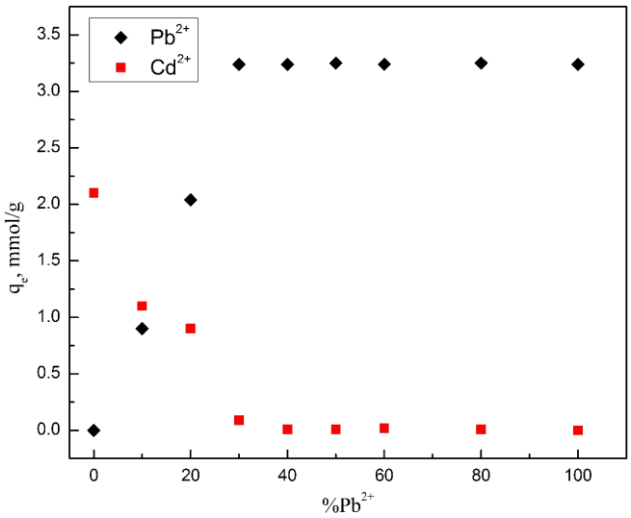

Figure 6 | Effect of Pb^{2+}-Cd^{2+} metal ratio on the selectivity of A-NMF adsorbent.

competitive Cd^{2+} ion. The highest Pb^{2+} concentration in this system (Cd^{2+}:Pb^{2+} = 8:2) is 2.2 mmol.L^{-1} and the corresponding adsorption capacity for Pb^{2+} at this concentration is 2.0 mmol.g^{-1}, which is below the saturation capacity. Initially, the adsorbent preferentially adsorbs the Pb^{2+} ions on the surface, and subsequently, the Cd^{2+} ions are adsorbed on the remaining available sites until saturation. It is notable that the added-up total capacity in this system is 3.1 mmol.g^{-1} which is in the same range as previously studied Pb^{2+}-dominated systems. The trend in this figure also indicates the reduction, but not inhibition, of Cd^{2+} adsorption by increasing the total metal concentration. When the molar ratio of the Pb^{2+} ions is further reduced to 10% of the total metal present in the solution, the added-up capacity is decreased to around 2 mmol.g^{-1}. It is due to the fact that at such a low Pb^{2+} concentration, the Cd^{2+} ions play the major role in determining the adsorption capacity. Because the maximum adsorption capacity of the adsorbent for Cd^{2+} is only 2.1 mmol.g^{-1}, the added-up capacity in such a low level of Pb^{2+} ions is similar to the single-component Cd^{2+} adsorption (see Figure 6).

pH effect

One of the most important parameters which affects the metal uptake capacity of adsorbent materials is the pH value of the metal solutions. The adsorption capacities of the material for Pb^{2+} and Cd^{2+} ions at various pH values in single- and binary-component systems are shown in Figure 8.

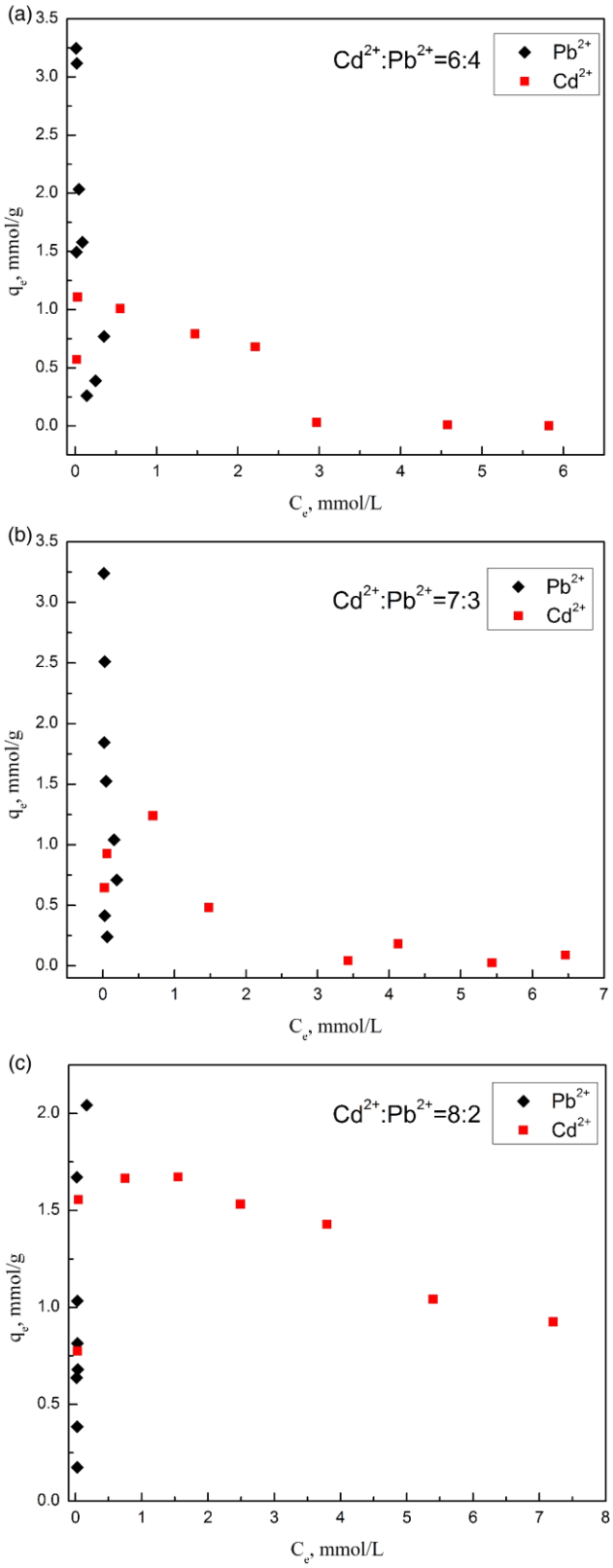

Figure 7 | Non-equimolar binary-component adsorption at metal ratios of (a) Cd^{2+}:Pb^{2+} = 6:4, (b) Cd^{2+}:Pb^{2+} = 7:3 and (c) Cd^{2+}:Pb^{2+} = 8:2.

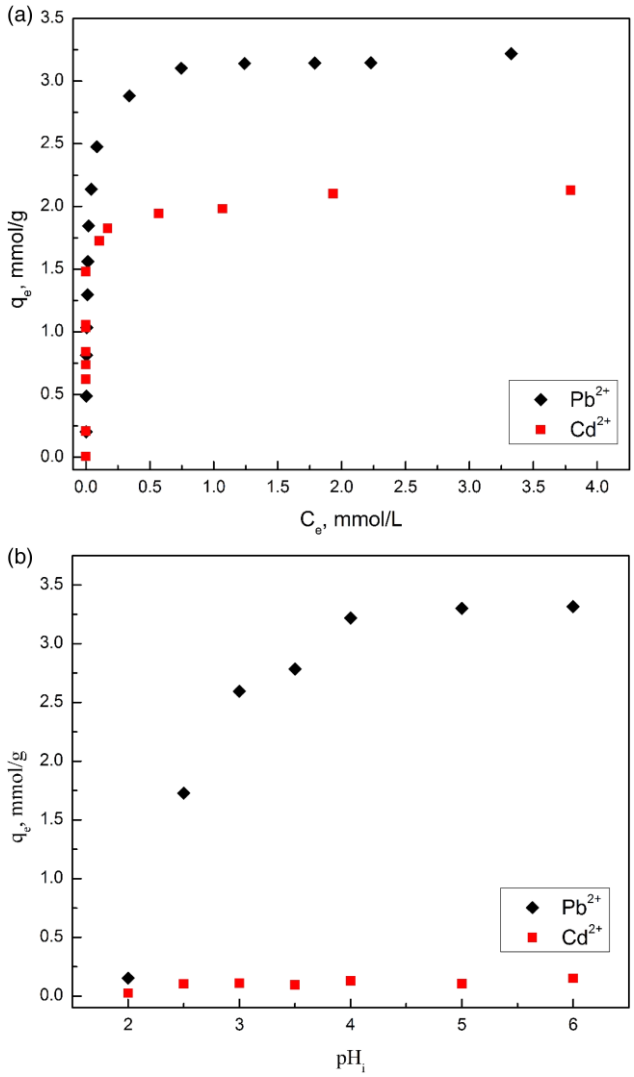

Figure 8 | pH effect for (a) single-component system and (b) binary-component system. Experimental conditions: 50 mL metal solution at initial metal concentration 6 mmol L^{-1}, initial pH = 2–6 mmol L^{-1}, Pb^{2+}:Cd^{2+} = 1 for binary, 0.05 g adsorbent, equilibrium time = 5 days.

In single-component systems, A-NMF uptakes trivial quantities of the metal ions at a very low pH value of 2. With an increase in the pH values of the solutions from 2 to 3.5, the metal adsorption capacities increase drastically. As the pH values are further increased above 3.5, the metal uptakes gradually reach a plateau. This trend has also been observed by other researchers (Pérez-Marín *et al.* 2007). This behavior is attributed to the competition between metal ions and hydrogen ions. At low pH values, the concentration of hydrogen ions present in the solution is sufficiently high to compete with the metal ions to occupy the available surface sites which leads to lower adsorption capacities. As the pH values of the solutions increase, the metal ions can easily capture the adsorption sites due to the lesser protonation of the surface sites, resulting in higher metal uptakes.

In the binary system, a complete selective behavior has been observed irrespective of the pH. The trend of change in the adsorption capacity of Pb^{2+} ions from the binary effluent is also similar to the single-component system. However, the Cd^{2+} ions are not adsorbed from the binary solution at any pH values. It is also interesting to note that, while some literature report the reduction in the adsorption capacity of the adsorbent in multi-component systems compared to the single-component solutions (Srivastava *et al.* 2006; Lam *et al.* 2007), the adsorption capacity of the adsorbent for Pb^{2+} ions does not change in the presence of Cd^{2+} ions, which can be highly advantageous.

The equilibrium pH values have been measured and all the results show that no precipitation occurs during the experiments.

CONCLUSION

In this work, single- and binary-component adsorptions for Pb^{2+} and Cd^{2+} ions using waste printed circuit board-based adsorbent (A-NMF) have been performed. Although the untreated material is incapable of adsorbing any metal ion, the activated material (A-NMF) has high adsorption capacities of 3.2 mmol.g^{-1} and 2.1 mmol.g^{-1} for Pb^{2+} and Cd^{2+}, respectively, in single component systems. The best fit model for both of the single-component adsorption systems has been found to be the Redlich–Peterson model. Since the power parameter in this model approaches unity, the adsorption mechanism of the metal ions has been proposed to be Langmuirian, indicative of monolayer adsorption on a homogeneous surface. Furthermore, A-NMF shows distinctive adsorption selectivity towards Pb^{2+} in a Pb^{2+}–Cd^{2+} equimolar binary-component system irrespective of the pH value of the metal solution. When the molar ratio of Pb^{2+} decreases to a threshold value of 30%, no significant change in selectiveness is observed. Further decrease in the Pb^{2+} molar ratio results in the simultaneous uptake of the two metals. This is attributed to the higher collision of the Cd^{2+} ions with the active adsorption sites due to higher accessibility of these ions. At Pb^{2+} molar ratio as low as 10%, the behavior of the system closely approaches that of the Cd^{2+} single-component system. Also, it has been demonstrated that the adsorption capacity of the adsorbent material for Pb^{2+} ions does not decrease in the binary-component system compared to

the single-component system, which can be of high significance in industrial applications.

ACKNOWLEDGEMENTS

The authors gratefully acknowledge the funding from the Hong Kong Research Grand Council. We would like to thank the Material Characterization and Preparation Facility at HKUST for the use of the equipment.

REFERENCES

Al-Duri, B., Khader, Y. & McKay, G. 1992 Prediction of binary component isotherms for adsorption on heterogeneous surfaces. *Journal of Chemical Technology & Biotechnology* **53** (4), 345–352.

Amuda, O. S., Giwa, A. A. & Bello, I. A. 2007 Removal of heavy metal from industrial wastewater using modified activated coconut shell carbon. *Biochemical Engineering Journal* **36** (2), 174–181.

Apiratikul, R. & Pavasant, P. 2008 Sorption of Cu^{2+}, Cd^{2+}, and Pb2+ using modified zeolite from coal fly ash. *Chemical Engineering Journal* **144** (2), 245–258.

Bradl, H. B. 2004 Adsorption of heavy metal ions on soils and soils constituents. *Journal of Colloid and Interface Science* **277** (1), 1–18.

Cheung, C. W., Chan, C. K., Porter, J. F. & McKay, G. 2001 Combined diffusion model for the sorption of cadmium, copper, and zinc ions onto bone char. *Environmental Science & Technology* **35** (7), 1511–1522.

Chiban, M., Soudani, A., Sinan, F. & Persin, M. 2011 Single, binary and multi-component adsorption of some anions and heavy metals on environmentally friendly Carpobrotus edulis plant. *Colloids and Surfaces B: Biointerfaces* **82** (2), 267–276.

Chuah, T. G., Jumasiah, A., Azni, I., Katayon, S. & Thomas Choong, S. Y. 2005 Rice husk as a potentially low-cost biosorbent for heavy metal and dye removal: an overview. *Desalination* **175** (3), 305–316.

Corami, A., Mignardi, S. & Ferrini, V. 2008 Cadmium removal from single- and multi-metal (Cd + Pb + Zn + Cu) Solutions by sorption on hydroxyapatite. *Journal of Colloid and Interface Science* **317** (2), 402–408.

Dąbrowski, A., Hubicki, Z., Podkościelny, P. & Robens, E. 2004 Selective removal of the heavy metal ions from waters and industrial wastewaters by ion-exchange method. *Chemosphere* **56** (2), 91–106.

Demirbas, A., Pehlivan, E., Gode, F., Altun, T. & Arslan, G. 2005 Adsorption of Cu(II), Zn(II), Ni(II), Pb(II), and Cd(II) from aqueous solution on Amberlite IR-120 synthetic resin. *Journal of Colloid and Interface Science* **282** (1), 20–25.

Duta, A. & Visa, M. 2015 Simultaneous removal of two industrial dyes by adsorption and photocatalysis on a fly-ash–TiO_2 composite. *Journal of Photochemistry and Photobiology A: Chemistry* **306**, 21–30.

El-Kamash, A. M., Zaki, A. A. & El Geleel, M. A. 2005 Modeling batch kinetics and thermodynamics of zinc and cadmium ions removal from waste solutions using synthetic zeolite, A. *Journal of Hazardous Materials* **127** (1–3), 211–220.

Entezari, M. H. & Soltani, T. 2009 Cadmium and lead ions can be removed simultaneously from a binary aqueous solution by the sono-sorption method. *Ultrasonics Sonochemistry* **16** (4), 495–501.

Fan, L., Luo, C., Sun, M., Li, X. & Qiu, H. 2013 Highly selective adsorption of lead ions by water-dispersible magnetic chitosan/graphene oxide composites. *Colloids and Surfaces B: Biointerfaces* **103**, 523–529.

Fritz, W. & Schlunder, E. 1981 Competitive adsorption of two dissolved organics onto activated carbon. Pt. 1: adsorption equilibria. *Chemical Engineering Science* **36** (4), 721–730.

Fu, F. & Wang, Q. 2011 Removal of heavy metal ions from wastewaters: A review. *Journal of Environmental Management* **92** (3), 407–418.

Gupta, V. K. & Ali, I. 2004 Removal of lead and chromium from wastewater using bagasse fly ash – a sugar industry waste. *Journal of Colloid and Interface Science* **271** (2), 321–328.

Hadi, P., Barford, J. & McKay, G. 2013a Synergistic effect in the simultaneous removal of binary cobalt–nickel heavy metals from effluents by a novel e-waste-derived material. *Chemical Engineering Journal* **228**, 140–146.

Hadi, P., Barford, J. & McKay, G. 2013b Toxic heavy metal capture using a novel electronic waste-based material – Mechanism, modeling and comparison. *Environmental Science & Technology* **47** (15), 8248–8255.

Hadi, P., Gao, P., Barford, J. P. & McKay, G. 2013c Novel application of the nonmetallic fraction of the recycled printed circuit boards as a toxic heavy metal adsorbent. *Journal of Hazardous Materials* **252–253**, 166–170.

Hadi, P., Barford, J. & McKay, G. 2014 Selective toxic metal uptake using an e-waste-based novel sorbent–Single, binary and ternary systems. *Journal of Environmental Chemical Engineering* **2** (1), 332–339.

Hadi, P., Xu, M., Lin, C. S. K., Hui, C.-W. & McKay, G. 2015a Waste printed circuit board recycling techniques and product utilization. *Journal of Hazardous Materials* **283**, 234–243.

Hadi, P., Ning, C., Ouyang, W., Xu, M., Lin, C. S. K. & McKay, G. 2015b Toward environmentally-benign utilization of nonmetallic fraction of waste printed circuit boards as modifier and precursor. *Waste Management* **35**, 236–246.

Horsfall Jr, M., Abia, A. A. & Spiff, A. I. 2006 Kinetic studies on the adsorption of Cd^{2+}, Cu^{2+} and Zn^{2+} ions from aqueous solutions by cassava (*Manihot sculenta* Cranz) tuber bark waste. *Bioresource Technology* **97** (2), 283–291.

Itskos, G., Koutsianos, A., Koukouzas, N. & Vasilatos, C. 2015 Zeolite development from fly ash and utilization in lignite mine-water treatment. *International Journal of Mineral Processing* **139**, 43–50.

Jo, Y.-H., Do, S.-H. & Kong, S.-H. 2014 Feasibility test for waste-reclaimed material to remove Cu^{2+} and Zn^{2+}: Kinetics and

applications to treat a real plating wastewater. *Journal of Environmental Chemical Engineering* **2** (1), 619–625.

Kabbashi, N. A., Atieh, M. A., Al-Mamun, A., Mirghami, M. E. S., Alam, M. D. Z. & Yahya, N. 2009 Kinetic adsorption of application of carbon nanotubes for Pb(II) removal from aqueous solution. *Journal of Environmental Sciences* **21** (4), 539–544.

Kadirvelu, K., Thamaraiselvi, K. & Namasivayam, C. 2001 Removal of heavy metals from industrial wastewaters by adsorption onto activated carbon prepared from an agricultural solid waste. *Bioresource Technology* **76** (1), 63–65.

Kadirvelu, K., Goel, J. & Rajagopal, C. 2008 Sorption of lead, mercury and cadmium ions in multi-component system using carbon aerogel as adsorbent. *Journal of Hazardous Materials* **153** (1–2), 502–507.

Karnitz Jr, O., Gurgel, L. V. A., de Melo, J. C. P., Botaro, V. R., Melo, T. M. S., de Freitas Gil, R. P. & Gil, L. F. 2007 Adsorption of heavy metal ion from aqueous single metal solution by chemically modified sugarcane bagasse. *Bioresource Technology* **98** (6), 1291–1297.

Kobya, M., Demirbas, E., Senturk, E. & Ince, M. 2005 Adsorption of heavy metal ions from aqueous solutions by activated carbon prepared from apricot stone. *Bioresource Technology* **96** (13), 1518–1521.

Kostova, I., Vassileva, C., Dai, S., Hower, J. C. & Apostolova, D. 2013 Influence of surface area properties on mercury capture behaviour of coal fly ashes from some Bulgarian power plants. *International Journal of Coal Geology* **116–117**, 227–235.

Lam, K. F., Yeung, K. L. & McKay, G. 2007 Efficient approach for Cd2+ and Ni2+ removal and recovery using mesoporous adsorbent with tunable selectivity. *Environmental Science & Technology* **41** (9), 3329–3334.

Larous, S., Meniai, A. H. & Lehocine, M. B. 2005 Experimental study of the removal of copper from aqueous solutions by adsorption using sawdust. *Desalination* **185** (1–3), 483–490.

Leyva-Ramos, R., Bernal-Jacome, L. A. & Acosta-Rodriguez, I. 2005 Adsorption of cadmium(II) from aqueous solution on natural and oxidized corncob. *Separation and Purification Technology* **45** (1), 41–49.

Li, Q., Zhai, J., Zhang, W., Wang, M. & Zhou, J. 2007 Kinetic studies of adsorption of Pb(II), Cr(III) and Cu(II) from aqueous solution by sawdust and modified peanut husk. *Journal of Hazardous Materials* **141** (1), 163–167.

Low, K. S., Lee, C. K. & Liew, S. C. 2000 Sorption of cadmium and lead from aqueous solutions by spent grain. *Process Biochemistry* **36** (1–2), 59–64.

Malandrino, M., Abollino, O., Giacomino, A., Aceto, M. & Mentasti, E. 2006 Adsorption of heavy metals on vermiculite: Influence of pH and organic ligands. *Journal of Colloid and Interface Science* **299** (2), 537–546.

Mavrov, V., Erwe, T., Blöcher, C. & Chmiel, H. 2003 Study of new integrated processes combining adsorption, membrane separation and flotation for heavy metal removal from wastewater. *Desalination* **157** (1–3), 97–104.

McKay, G. & Al-Duri, B. 1991 Extended empirical Freundlich isotherm for binary systems: a modified proce dure to obtain the correlative constants. *Chemical Engineering and Processing: Process Intensification* **29** (3), 133–138.

Memon, S. Q., Memon, N., Shah, S. W., Khuhawar, M. Y. & Bhanger, M. I. 2007 Sawdust – A green and economical sorbent for the removal of cadmium (II) ions. *Journal of Hazardous Materials* **139** (1), 116–121.

Mohan, D. & Singh, K. P. 2002 Single- and multi-component adsorption of cadmium and zinc using activated carbon derived from bagasse – an agricultural waste. *Water Research* **36** (9), 2304–2318.

Momčilović, M., Purenović, M., Bojić, A., Zarubica, A. & Ranđelović, M. 2011 Removal of lead(II) ions from aqueous solutions by adsorption onto pine cone activated carbon. *Desalination* **276** (1–3), 53–59.

Noeline, B. F., Manohar, D. M. & Anirudhan, T. S. 2005 Kinetic and equilibrium modelling of lead(II) sorption from water and wastewater by polymerized banana stem in a batch reactor. *Separation and Purification Technology* **45** (2), 131–140.

Norris, P., Hagan, S., Cohron, M., Zhao, H., Pan, W.-P. & Li, K. 2015 Application of fly ash as an adsorbent for Estradiol in animal waste. *Journal of Environmental Management* **161**, 57–62.

Ogata, F., Iwata, Y. & Kawasaki, N. 2015 Properties of novel adsorbent produced by hydrothermal treatment of waste fly ash in alkaline solution and its capability for adsorption of tungsten from aqueous solution. *Journal of Environmental Chemical Engineering* **3** (1), 333–338.

Özer, A. & Pirinççi, H. B. 2006 The adsorption of Cd(II) ions on sulphuric acid-treated wheat bran. *Journal of Hazardous Materials* **137** (2), 849–855.

Pang, Y., Zeng, G., Tang, L., Zhang, Y., Liu, Y., Lei, X., Li, Z., Zhang, J. & Xie, G. 2011 PEI-grafted magnetic porous powder for highly effective adsorption of heavy metal ions. *Desalination* **281**, 278–284.

Pant, D. & Singh, P. 2013 Chemical modification of waste glass from cathode ray tubes (CRTs) as low cost adsorbent. *Journal of Environmental Chemical Engineering* **1** (3), 226–232.

Pérez-Marín, A. B., Zapata, V. M., Ortuño, J. F., Aguilar, M., Sáez, J. & Lloréns, M. 2007 Removal of cadmium from aqueous solutions by adsorption onto orange waste. *Journal of Hazardous Materials* **139** (1), 122–131.

Pizarro, J., Castillo, X., Jara, S., Ortiz, C., Navarro, P., Cid, H., Rioseco, H., Barros, D. & Belzile, N. 2015 Adsorption of Cu^{2+} on coal fly ash modified with functionalized mesoporous silica. *Fuel* **156**, 96–102.

Qiu, W. & Zheng, Y. 2009 Removal of lead, copper, nickel, cobalt, and zinc from water by a cancrinite-type zeolite synthesized from fly ash. *Chemical Engineering Journal* **145** (3), 483–488.

Rouquerol, F., Rouquerol, J. & Sing, K. 1999 Chapter 5 - Adsorption at the liquid-solid interface: Thermodynamics and methodology. In: *Adsorption by Powders and Porous Solids* (F. Rouquerol, J. Rouquerol & K. Sing, eds). Academic Press, London, pp. 117–163.

Sang, Y., Li, F., Gu, Q., Liang, C. & Chen, J. 2008 Heavy metal-contaminated groundwater treatment by a novel nanofiber membrane. *Desalination* **223** (1–3), 349–360.

Shih, W.-H. & Chang, H.-L. 1996 Conversion of fly ash into zeolites for ion-exchange applications. *Materials Letters* **28** (4–6), 263–268.

Sočo, E. & Kalembkiewicz, J. 2013 Adsorption of nickel(II) and copper(II) ions from aqueous solution by coal fly ash. *Journal of Environmental Chemical Engineering* **1** (3), 581–588.

Srivastava, V. C., Mall, I. D. & Mishra, I. M. 2006 Equilibrium modelling of single and binary adsorption of cadmium and nickel onto bagasse fly ash. *Chemical Engineering Journal* **117** (1), 79–91.

Taghi ganji, M., Khosravi, M. & Rakhshaee, R. 2005 Biosorption of Pb, Cd, Cu and Zn from the wastewater by treated Azolla filiculoides with H_2O_2/$MgCl_2$. *International Journal of Environmental Science & Technology* **1** (4), 265–271.

Tiemann, K. J., Gamez, G., Dokken, K., Parsons, J. G. & Gardea-Torresdey, J. L. 2002 Chemical modification and X-ray absorption studies for lead(II) binding by *Medicago sativa* (alfalfa) biomass. *Microchemical Journal* **71** (2–3), 287–293.

Veli, S. & Alyüz, B. 2007 Adsorption of copper and zinc from aqueous solutions by using natural clay. *Journal of Hazardous Materials* **149** (1), 226–233.

Wan Ngah, W. S. & Hanafiah, M. A. K. M. 2008 Removal of heavy metal ions from wastewater by chemically modified plant wastes as adsorbents: A review. *Bioresource Technology* **99** (10), 3935–3948.

Wang, C.-F., Li, J.-S., Wang, L.-J. & Sun, X.-Y. 2008 Influence of NaOH concentrations on synthesis of pure-form zeolite A from fly ash using two-stage method. *Journal of Hazardous Materials* **155** (1–2), 58–64.

Wong, K. K., Lee, C. K., Low, K. S. & Haron, M. J. 2003 Removal of Cu and Pb from electroplating wastewater using tartaric acid modified rice husk. *Process Biochemistry* **39** (4), 437–445.

Xu, M., Hadi, P., Chen, G. & McKay, G. 2014 Removal of cadmium ions from wastewater using innovative electronic waste-derived material. *Journal of Hazardous Materials* **273**, 118–123.

Yalçinkaya, Y., Arica, M. Y., Soysal, L., Denizli, A., Genç, O. & Bektaş, S. 2002 Cadmium and mercury uptake by immobilized *Pleurotus sapidus*. *Turkish Journal of Chemistry* **26**, 441–452.

Yang, G., Tang, L., Lei, X., Zeng, G., Cai, Y., Wei, X., Zhou, Y., Li, S., Fang, Y. & Zhang, Y. 2014 Cd(II) removal from aqueous solution by adsorption on α-ketoglutaric acid-modified magnetic chitosan. *Applied Surface Science* **292**, 710–716.

Yuan, S., Chen, X.-L., Li, J. & Wang, F.-C. 2011 CO_2 Gasification kinetics of biomass char derived from high-temperature rapid pyrolysis. *Energy & Fuels* **25** (5), 2314–2321.

Zhou, C., Gao, Q., Luo, W., Zhou, Q., Wang, H., Yan, C. & Duan, P. 2015 Preparation, characterization and adsorption evaluation of spherical mesoporous Al-MCM-41 from coal fly ash. *Journal of the Taiwan Institute of Chemical Engineers* **52**, 147–157.

First received 29 May 2015; accepted in revised form 5 August 2015. Available online 19 August 2015